CrossMark

ORIGINAL PAPER

Preparation of orange-red fluorescent gold nanoclusters using denatured casein as a reductant and stabilizing agent, and their application to imaging of HeLa cells and for the quantitation of mercury(II)

Shouming Xu[1] · Hong Yang[2] · Kang Zhao[1] · Jianguo Li[1] · Liyun Mei[1] · Yun Xie[1] ·
Anping Deng[1]

Abstract We describe a method for the preparation of water-soluble gold nanoclusters (Au-NCs) from chloroauric acid using denatured-casein as both a reducing and stabilizing agent. The resulting Au-NCs were characterized by photoluminescence, UV–vis absorption, and X-ray photoelectron spectroscopies, and by transmission electron microscopy. The Au-NCs have an average diameter of 1.7 ± 0.2 nm and exhibit orange-red fluorescence emission peaking at 600 nm (with a Stokes' shift as large as 237 nm), a quantum yield of 4.3 %, and good stability over the physiologically relevant range of pH values and ionic strength. Cytotoxicity studies showed the Au-NCs to display negligible effects in terms of altering cell proliferation or triggering apoptosis. Fluorescence imaging of HeLa cancer cells was accomplished by loading such cells with the Au-NCs. The fluorescence of the Au-NCs is found to be strongly quenched by Hg(II) ions, and thus the Au-NCs can be used for detecting and, possibly, imaging of Hg(II). An assay was worked out for the determination of Hg(II), and its limit of detection is 1.83 nM, which is 5.5 times lower than the maximum allowed concentration of Hg(II) in drinking water as defined by the US EPA.

Introduction

Luminescence techniques have experienced rapid development and emerged as vital tools in the area of chemical and biochemical analysis [1–3]. Some fluorescent nanomaterials such as semiconductor quantum dots [2], polymer dots [4], metal nanoclusters [5, 6], carbon-based quantum dots [1] and rare earth material [3] have been widely used in chemical and biochemical analysis. Currently, considerable research efforts are directed towards synthesizing metal nanoclusters (Au, Ag and Cu) due to their unique photo-physical properties and possible application in cellular and tissue imaging [7–12]. Among them, gold nanoclusters (Au-NCs) as fluorescence probes have drawn wide attention because they have ultra-small sizes, large Stokes shift, low toxicity, strong fluorescence and good stability [5, 6]. Therefore, it is of great significance to facilely synthesize the Au-NCs and further broaden their application as a promising bioprobe.

Many methods have been developed for the synthesis of Au-NCs such as by chemical reduction [13], photochemical reduction [14], phase-transfer [15], chemical etching of metallic nanoparticles [16], and transformation from other metal nanoclusters via galvanic replacement reaction [17]. In these methods, chemical reduction is supposed to be the most general route for the preparation

✉ Jianguo Li
lijjgsd@suda.edu.cn

✉ Anping Deng
denganping@suda.edu.cn

1 The Key Lab of Health Chemistry & Molecular Diagnosis of Suzhou, College of Chemistry, Chemical Engineering and Materials Science, Soochow University, Suzhou 215123, China

2 College of Pharmacy Sciences, Soochow University, Suzhou 215123, China

of Au-NCs, in which a variety of different templates including dendrimers, polyelectrolytes, thiol-containing molecules, DNA, peptides, and proteins are utilized [13, 18–35]. Among them, protein-directed synthesis is particularly attractive, because proteins contain many active sites such as thiol, amino, hydroxyl, and carboxyl to accumulate and reduce Au^{3+} ions, and can also act as the stabilizer of Au-NCs [13, 18, 19, 26–36]. So far, many proteins have been used for the synthesis of Au-NCs, including lsyzoyme type VI [26], horseradish peroxidase [27], insulin [28], bovine serum albumin [13, 29, 30], human transferrin [31], lactoferrin [32], tryspin [33], pepsin [34], papain [35], human adult hemoglobin [36]. Although there are many reports about protein-directed synthesis of Au-NCs, however up to now, there is no report using casein as a reducing/stabilizing reagent for the preparation of Au-NCs.

Casein is the name for a family of related phosphoproteins (αS1, αS2, β, κ), and contains a fairly high number of proline residues. Recently, Ma's group [37] reported a facile one-pot synthesis of L-proline-stabilized fluorescent Au-NCs, which exhibited bluish fluorescence emission at 440 nm and a quantum yield of 2.94 %. Inspired by that report, we thought the casein which is rich in proline residues might be a good candidate protein for the preparation Au-NCs.

Mercury (Hg^{2+}) is highly toxic and has bio-accumulative properties [38], The maximum allowed concentration of Hg^{2+} in drinking water is 10 nM according to United States Environment Protection Agency [39]. Thus it is necessary to develop mercury detectors for both environmental and biological samples. Recently, due to the features of high sensitivity, facile operation, real time and online detection, fluorescence detection has become more and more popular. Metal nanoparticle-based probes are useful for the fast and ultrasensitive fluorescence detection of Hg^{2+} ions [40–45]. As a member of fluorescent metal nanoparticles, Au-NCs have also been utilized as Hg^{2+} probes based on the quenching of their fluorescence [26, 46–49], Nevertheless, it is still a challenge to develop more simple, fast, high selective and sensitive methods for mercury detection.

Herein, we reported a simple and fast one-pot synthesis of Au-NCs by reducing chloroauric acid using denatured-casein as a reducing/stabilizing reagent. The Au-NCs possess fluorescence emission (600 nm) and display non-cytotoxicity and excellent biocompatibility on human cervical carcinoma (HeLa) cancer cells. In addition, it was observed that the fluorescence of the Au-NCs is quenched by Hg^{2+}. Thus, the Au-NCs can be used as a fluorescent probe for the determination of Hg^{2+} ions.

Experimental

Reagents and materials

All chemicals used were of analytical grade and were used as received without further purification. Rhodamine 6G and gold (III) chloride tetrahydrate ($HAuCl_4 \cdot 4H_2O$) were purchased from Sinopharm Chemical Reagent Co., Ltd (Shanghai, China, www.sinoreagent.com). Casein and mercuric chloride ($HgCl_2$) were purchased from Sigma-Aldrich (Milwaukee, USA, www.sigma-aldrich.com). Mercury stock solution (1 mg mL^{-1}) was prepared by dissolving 6.77 mg $HgCl_2$ in 5 mL of 2 % (v/v) HNO_3 and kept at 4 °C. In all preparations, high-purity deionized water (18.2 MΩ cm) from a Dura series (The Lab Corporation, USA) was used. The other metal salts used here were also obtained from Sinopharm Chemical Reagent Co., Ltd (Shanghai, China, www.sinoreagent.com).

Instruments

UV–vis absorption spectra were recorded with a spectrophotometer UV-2300 (Techcomp., Shanghai, China, www.techcomp.cn), and fluorescence spectra were taken on a spectrofluorometer F-2500 (Hitachi, Japan, www.hitachi.com.cn). Transmission electron microscopy (TEM) was performed on a FEI Tecnai G-20 (FEI, Eindhoven, Netherlands, www.fei.com), which was operated at an accelerating voltage of 200 kV. TEM samples were prepared by spraying a dispersion of Au-NCs onto a Cu grid covered by a holey carbon film. X-Ray photoelectron spectroscopy (XPS) measurements were carried out on a K-Alpha XPS spectrometer (ThermoFisher, E. Grinstead, UK, www.thermo.com.cn) , using Al Ka X-ray radiation (1486.6 eV) for excitation. The cellular fluorescence images were recorded by TCS SP5 II Confocal laser scanning microscope (Leica, Germany, www.leica.com).

Synthesis of denatured casein protected Au-NCs

All glassware used in the experiment was cleaned in a bath of freshly prepared aqua regia (HCl : HNO_3, 3 : 1 by volume) and rinsed thoroughly in water prior to use. In a typical experiment, 0.5 g casein with 100 mL 0.01 mol L^{-1} phosphate buffered solution (PBS) was boiled for 10 min so that the casein was completely dissolved and denaturized. The solution was cooled down to room temperature. Then to 6 mL of the casein solution (0.5 % by mass), 0.075 mL aqueous $HAuCl_4$ solution (1 % by mass) was added. The mixture was incubated at 90 °C under vigorous stirring for 3 min,

then 0.2 mL 1 mol L^{-1} NaOH solution was added. The mixture was further incubated at 90 °C for 30 min. The as-prepared Au-NCs were puried by dialysis, using dialysis tube with a molecular weight cut-off of 8 kDa to remove impurities and stored at 4 °C until use.

Cell culture and viability

Human cervical carcinoma (HeLa) cells were cultured in Dulbecco's modified eagle medium (DMEM), supplemented with 10 % fetal calf serum (FCS, Gibco BRL), 100 U of penicillin, and 100 U of streptomycin in a humidified incubator at 37 °C and 5 % CO$_2$. Prior to being tested, cells were seeded in 96 well plates (Gibco BRL) at an initial density of 1×10^5 cells per mL for 24 h. Dilutions of the Au-NCs were then added to DMEM medium and incubated for another 24 h. Afterwards, cells were washed twice with PBS followed by addition of 100 μL fresh medium and 20 μL 3-(4,5-dimethylthiazol-2-yl)-2,5-diph-eny-2 h-tetrazoliumbromide (MTT, Sigma) stock suspension (5 mg mL^{-1}) to each well. They were incubated for 4 h at 37 °C and 5 % CO$_2$. After removing all from the wells, 150 μL dimethylsulfoxide (DMSO) was added to each well. The solution in the well was mixed thoroughly and incubated at 37 °C for 10 min. The absorbance at 490 nm was measured with an enzyme mark instrument (Sunrise Remote, Tecan, Austria). The viability of the HeLa cells exposed to the Au-NCs was expressed as a relative percentage as normalized to the untreated control which was set as 100 %. All the records were explained as average data with error bars.

Cell imaging

The cellular uptake of the Au-NCs was studied by confocal laser scanning microscope. Typically, HeLa cells were cleaved by trypsin, seeded, and grown onto 18 mm glass coverslips in a 6-well culture plate for 24 h. After an appropriate incubation time (3 h) with 50 μM of Au-NCs, cells were washed three times with PBS, fixed with 4 % p-formaldehyde for 30 min, and mounted on microscope slides for fluorescence imaging.

Fluorescence assay of Hg^{2+}

Hg^{2+} standard solutions in the concentration range of 8 nM to 10,000 nM were prepared by diluting stock solution with pure water. In fluorescence probing Hg^{2+}, equal volume (500 μL individually) of the Au-NCs and (5 μL individually) Hg^{2+} was mixed thoroughly. After 5 min, the mixed solutions were transferred into a 0.75 mL quartz cuvette. Their fluorescence spectra of the Au-NCs after mixing with Hg^{2+} were recorded by fluorescence spectrophotometer at an excitation wavelength of 363 nm.

Results and discussion

Optimization of synthesizing Au-NCs

Fluorescent Au-NCs was prepared in one step by reducing gold salt with casein. The experiment conditions such as the amount of HAuCl$_4$, casein and NaOH utilized, the reaction time and temperature, etc. were carefully optimized. The detailed optimization was presented in Electronic Supplemental Material (ESM). From Fig. S1, the optimal conditions for Au-NCs preparation were found to be: 75 μl of HAuCl$_4$ solution (1 % by mass) was mixed with 6 mL of denatured casein solution (0.5 % by mass) and incubated at 90 °C under vigorous stirring for 3 min, then 0.2 mL 1 mol L^{-1} NaOH solution was introduced, and the mixture was further incubated at 90 °C for 30 min. Here, denatured casein acted as both a reductant and a stabilizer. NaOH was used to increase the pH value of the reaction solution (pH≥10) to improve the reducing power of denatured casein and thus accelerate the reduction of Au^{3+} into Au^0 [13, 14]. After reaction, an orange-red fluorescence was observed via irradiation of the light green product with a UV lamp. The obtained yellowish Au-NCs solution was used for subsequent characterization and applications.

Characterization of the Au-NCs

The fluorescence spectra of the Au-NCs was recorded and showed an excitation and emission maximum at 363 and 600 nm (Fig. 1a), respectively. The Stokes shift achieved with the Au-NCs is 237 nm, which is much larger than that obtained in literature [37] using L-proline-stabilized as reducing/stabilizing reagent for the preparation of Au-NCs with the Stokes shift value only of 75 nm. The emission band of our Au-NCs was observed in the orange-red spectral region from the photos of the Au-NCs solution under UV light irradiation and by the bare eye (Fig. 1b, inset). The UV/Vis spectra of the Au-NCs solution missed the characteristic surface plasmon absorption of gold nanoparticles at 520 nm [50]. Instead, it exhibited absorptions around 200–400 nm (Fig. 1b). For comparison, the absorption of pure HAuCl$_4$ solution was recorded and no absorption peak position of HAuCl$_4$ was observed in the absorption spectrum of the Au-NCs, which meant the reduction of Au^{3+}.
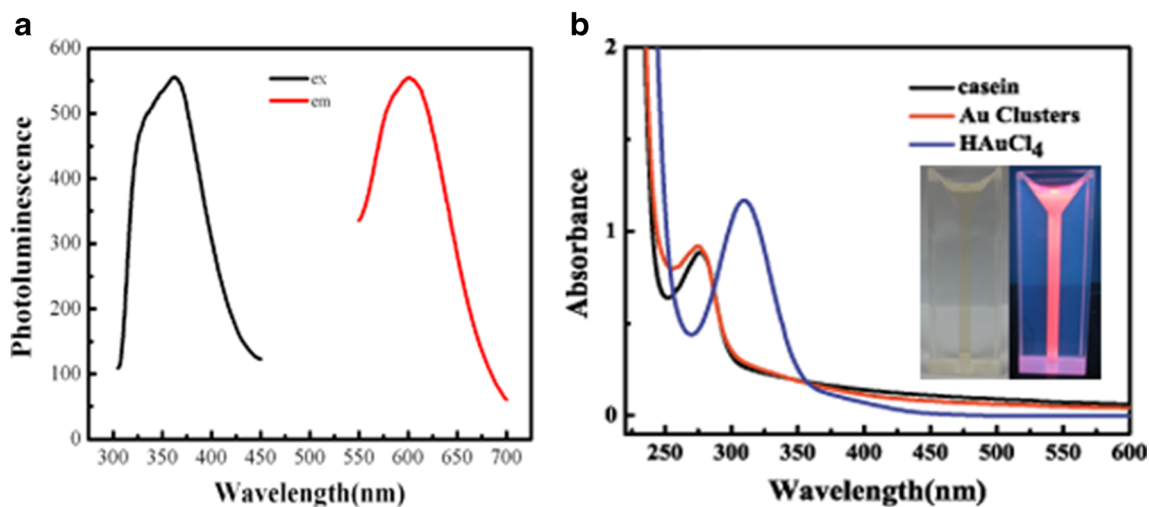
Fig. 1 **a** Fluorescence/excitation spectra of Au-NCs in water. Excitation spectrum (black line) recorded at λem=600 nm and fluorescence (red line) by excitation at λex=363 nm. **b** UV–vis absorption spectra of Au-NCs in water (red line), the HAuCl$_4$ solution (blue line), and the denatured casein solution (black line) and (inset) photographs of Au-NCs solution under visible light and under UV light

In the transmission electron microscopy (TEM) image of the Au-NCs in Fig. 2a, the nanoclusters are well dispersed, and aggregates are absent. The mean diameter of the Au-NCs was determined as 1.7±0.2 nm, as judged from over 100 individual particles. Their smaller size in comparison to other luminescent nanomaterials such as semiconductor QDs, rare earth up-converting nanoparticles and dye-doped silica nanoparticles makes these Au-NCs attractive as fluorescence imaging or probe.

To analyze the valence states of gold in the obtained Au-NCs, we carried out X-ray photoelectron spectroscopy (XPS) measurements to investigate the oxidation states of their surfaces. The Au4f XPS spectrum (Fig. 2b) shows the binding energy (BE) of Au4f7/2 and Au4f5/2 at 83.9 and 87.4 eV, respectively, suggesting that both Au^0 and Au$^+$ exist in the luminescent Au-NCs [17]. This phenomenon supports the hypothesis that a fraction of the gold atoms in luminescent Au-NCs exist in the Au (I) oxidation state, consistent with previously reported literature [13, 14, 17].

Using Rhodamine 6G (QY=95 % in ethanol) as the reference, the quantum yield of our luminescent Au-NCs in aqueous solution (pH 7.0) was measured to be 4.3 %. Obviously, the quantum yield achieved in this study was higher than that in Ma's report [37] with the quantum yield value of 2.94 % using L-proline-stabilized as reducing/stabilizing reagent for the preparation of Au-NCs. The strong brightness of the Au-NCs is an advantage as fluorescent probes in cellular imaging or probing.

The colloidal stability of the Au-NCs was also characterized quantitatively by measuring their fluorescence

Fig. 2 **a** Typical TEM image of Au-NCs, **b** XPS spectra showing the binding energy of Au4f of Au-NCs
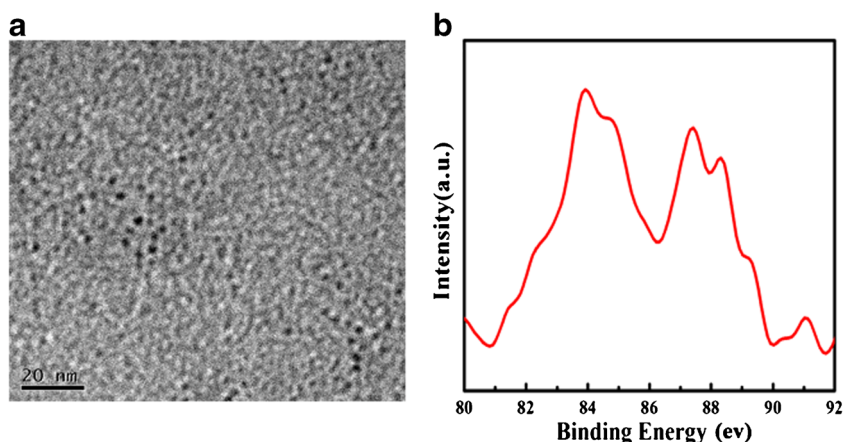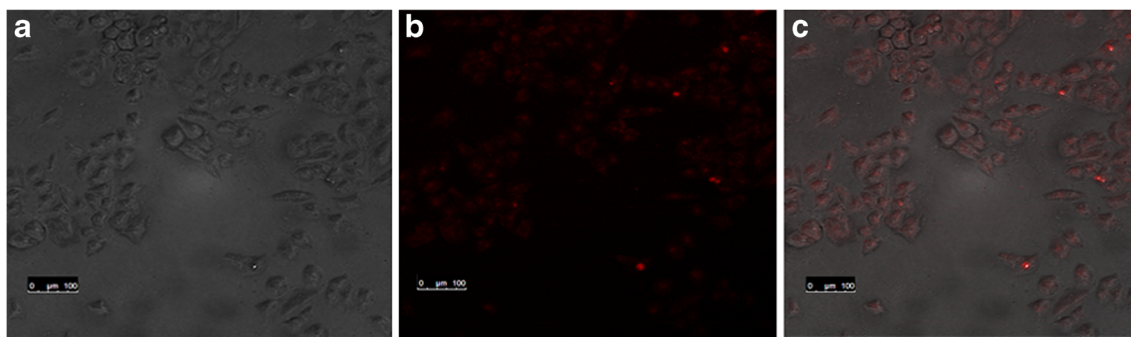
Fig. 3 Bright field images (**a**), Confocal fluorescence images (**b**) and the overlay of fluorescence and bright field images (**c**) of HeLa cells upon 3 h incubation with Au-NCs. Fluorescence images were taken with 405 nm excitation. Scale bar: 100 μm

intensity in PBS over a wide pH range and in KCl solution with different ionic strengths. As shown in Fig. S2, the fluorescence intensities of Au-NCs have less changeable between pH 3 and 9, are very stable in high-ionic strength solutions, implying that these nanoclusters possess a good colloidal stability over the entire physiologically relevant pH range and ionic strength. Such a good colloidal stability is particularly beneficial for biological applications.

Cellular imaging applications

Although ultra-small Au-NCs are generally considered nontoxic owing to their minimal metal content and the chemical inertness of Au [51], it is important to test their cytotoxicity to explore potential applications as optical probes in the life sciences. The cytotoxicity of the obtained luminescent Au-NCs was assessed via MTT assay after incubation for 24 h with HeLa cells observed that cell viability was greater than 85 % after incubation with Au-NCs in the concentration range of

0–300 μg mL^{-1} for 24 h (Fig. S3), indicating that these Au-NCs indeed have a low cytotoxicity.

Cellular imaging applications

To further investigate the potential application for the presented Au-NCs as luminescent probes in biological imaging, we then tested the imaging capability of the obtained luminescent Au-NCs by using HeLa cells. After incubation of 3 h with Au-NCs, cells were imaged by using confocal microscopy (Fig. 3). The emission luminescence from the Au-NCs can be clearly observed, and the luminescence signals suggest that the luminescent gold NPs were bonding to the cell membrane and that some of them had been ingested by the HeLa cells.

Fluorescence assay of Hg^{2+}

It has been reported that BSA-[42], lysozyme-[26] or trypsin-Stabilized [33] fluorescent Au-NCs can be used as sensitive and selective probes of metal ions such as Hg^{2+} ions through

Fig. 4 **a** Quenching of the PL (at λ$_{exc}$ of 363 nm) of the Au-NCs by Hg^{2+} ions present in 0, 8, 15, 20, 30, 40, 80, 150, 300, 500, 1000, 5000 and 10,000 nM concentration. **b** The Stern-Volmer plot in the linear detection range for 8–40 nM of Hg^{2+}
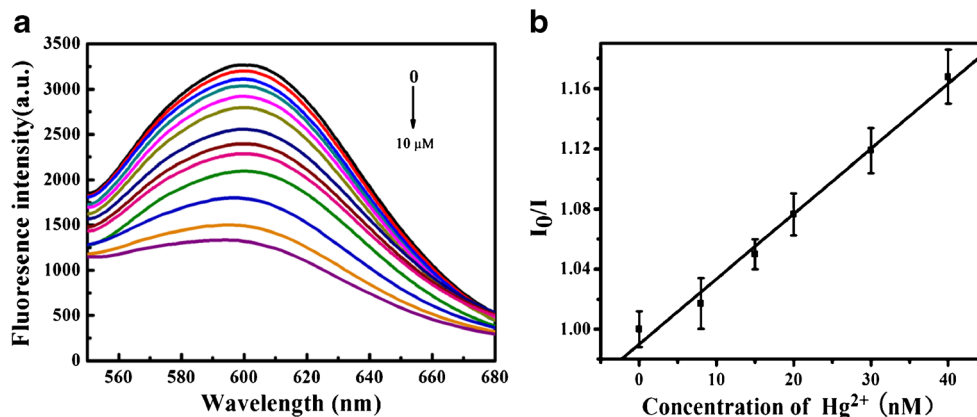
Table 1 Comparison of recently reported methods for determination of Hg^{2+} based on different protein-protected Au-NCs as probes

Probe	DLR^a	LOD^a	Comments	Ref.
BSA-Au-NCs	0.4–43.2 μM	80 nM	RSD*: 1.4 %, pH: 7.4, Selectivity, good (14 cations), Photostability, NR*, Response time: NR; Real sample: (river, tap, mineral) water	[49]
BSA-Au-NCs	1–20 nM	0.5 nM	RSD: NR, pH: NR, Selectivity, good (15 cations), Photostability, NR, Response time: NR; Real sample: NR	[47]
Lysozyme-Au-NCs	1–600 nM	3 pM	RSD: NR, pH: NR, Selectivity, good (18 cations), Photostability, NR, Response time: 10 min; Real sample: seawater	[26]
Casein-Au-NCs	8–40 nM	1.83 nM	RSD: NR, pH: NR, Selectivity, good (15 cations), Photostability, good, Response time: 5 min; Real sample: NR	this work

^{a} *DLR* dynamic linear range, *LOD* limit of detection, *RSD* relative standard deviation, *NR* not reported

fluorescence quenching by the Hg^{2+}-Au$^+$ interaction. Here, the effect of metal ion addition on the fluorescence intensity of the Au-NCs was investigated in the presence of 10 μM of Cu^{2+}, Ni^{2+}, Ca^{2+}, Mg^{2+}, Na$^+$, Pb^{2+}, Hg^{2+}, Zn^{2+}, Co^{2+}, Cd^{2+}, K$^+$, Ba^{2+}, Fe^{2+}, Fe3$^+$, Li$^+$. Fig. S4 shows the relative fluorescence (I/I$_0$) in the presence of 10 μM of the above metal ions. Only the addition of the Hg^{2+} ion resulted in the dominant quenching of the fluorescence of the Au-NCs, although there was a slight quenching of fluorescence in the presence of other metal ions such as Fe^{2+} and Ni^{2+}. Obviously, the fluorescence of the Au-NCs is strongly quenched by Hg^{2+}. Similar to BSA-, trypsin- or lysozyme-stabilized fluorescent Au-NCs for ions detection, the Au-NCs prepared in this study can be used for determination of Hg^{2+}. During the reaction, we found that the Hg^{2+}-induced fluorescence quenching of the Au-NCs reached nearly completion within 5 min (Fig. S5). As observed in Fig. 4a and Fig. S6, the fluorescence intensity of the Au-NCs decreased upon increasing the concentration of Hg^{2+}. The fluorescence intensity decreased linearly over the Hg^{2+} concentration range of 8–40 nM (Fig. 4b). The limit of detection (LOD) for Hg^{2+} ions was estimated to be 1.83 nM (S/N>3).

A comparison of some recently reported methods for determination of Hg^{2+} based on different protein-protected Au-NCs as probes is presented in Table 1. The parameters for comparison included linear dynamic range (LDR), limit of detection (LOD), effect of pH value, photostability, selectivity and response time, etc. It can be seen from Table 1 that although the LOD value of our Au-NCs probe is not the lowest, it is still 5.5 times lower than the maximum allowed concentration of Hg^{2+} in drinking water according to United States Environment Protection Agency [39]. Also our Au-NCs probe possessed other advantages such as simplicity, relatively cheap, short response time, good selectivity and high photostability, etc. The above results indicate that the fluorescence of the Au-NCs is particularly quenched by Hg^{2+}, and therefore the Au-NCs can be used as probes for high sensitive and selective detection of Hg^{2+}.

Conclusion

We have presented a straightforward one-pot approach to synthesize high fluorescent Au-NCs using denatured casein as both a reducing and a stabilizing agent. The obtained Au-NCs have small sizes, high fluorescence QY, non-toxicity, and good stability in biological media, and have been successful used as luminescent probes for bioimaging and fluorescence probes for high selectivity and sensitivity for the detection of Hg^{2+} in aqueous solution and the corresponding LOD was 1.83 nM. We are quite optimistic about this novel material can be extended to be used in other fields and the advantages of low cost and ease-of-synthesis would potentially lead the promising of further exploration of other naturally available proteins as the starting materials for the generation of the Au-NCs.

References

1. Luo PJG, Yang F, Yang ST, Sonkar SK, Yang LJ, Broglie JJ, Liua Y, Sun YP (2014) Carbon-based quantum dots for fluorescence imaging of cells and tissues. RSC Adv 4:10791

2. Wu P, Zhao T, Wang SL, Hou XD (2014) Semicondutor quantum dots-based metal ion probes. Nanoscale 6:43

3. Gai SL, Li CX, Yang PP, Lin J (2014) Recent progress in rare earth micro/nanocrystals: soft chemical synthesis, luminescent properties, and biomedical applications. Chem Rev 114:2343

4. Feng LH, Zhu CL, Yuan HX, Liu LB, Lv FT, Wang S (2013) Conjugated polymer nanoparticles: preparation, properties, functionalization and biological applications. Chem Soc Rev 42:6620

5. Zhang LB, Wang EK (2014) Metal nanoclusters: new fluorescent probes for sensors and bioimaging. Nano Today 9:132

6. Shang L, Dong SJ, Nienhaus GU (2011) Ultra-small fluorescent metal nanoclusters: synthesis and biological applications. Nano Today 6:401

7. Raut S, Rich R, Akopova I, Thyrhaug E, Shtoyko T, Shumilov D, Gryczynski Z, Gryczynski I (2012) Fluorescent polyelectrolyte capped silver nanoclusters: optimization and spectroscopic evaluation. Chem Phys Lett 549:72

8. Qian HF, Zhu MZ, Wu ZK, Jin RC (2012) Quantum sized gold nanoclusters with atomic precision. Acc Chem Res 45:1470

9. Xu HX, Suslick KS (2010) Water-soluble fluorescent silver nanoclusters. Adv Mater 22:1078

10. Lu YZ, Chen W (2012) Sub-nanometre sized metal clusters: from synthetic challenges to the unique property discoveries. Chem Soc Rev 41:3594

11. Retnakumari A, Setua S, Menon D, Ravindran P, Muhammed H, Pradeep T, Nair S, Koyakutty M (2010) Molecular-receptor-specific, non-toxic, near-infrared-emitting Au cluster-protein nanoconjugates for targeted cancer imaging. Nanotechnology 21: 055103

12. Durgadas CV, Sharma CP, Sreenivasan K (2011) Fluorescent gold clusters as nanosensors for copper ions in live cells. Analyst 136: 933

13. Xie JP, Zheng YG, Ying JY (2009) Protein-directed synthesis of highly fluorescent gold nanoclusters. J Am Chem Soc 131:888

14. Zhang H, Huang X, Li L, Zhang G, Hussain I, Li Z, Tan B (2012) Photoreductive synthesis of water-soluble fluorescent metal nanoclusters. Chem Commun 48:567

15. Yuan X, Luo ZT, Zhang QB, Zhang XH, Zheng YG, Lee JY, Xie JP (2011) Synthesis of highly fluorescent metal (Ag, Au, Pt, and Cu) nanoclusters by electrostatically induced reversible phase transfer. ACS Nano 5:8800

16. Shibu ES, Radha B, Verma PK, Bhyrappa PG, Kulkarni U, Pal SK, Pradeep T (2009) Functionalized Au22 clusters: synthesis, characterization, and patterning. ACS Appl Mater Inter 10:2199

17. Wang C, Wang Y, Xu L, Shi X, Li X, Xu X, Sun H, Yang B, Lin Q (2013) A galvanic replacement route to prepare strongly fluorescent and highly stable gold nanodots for cellular imaging. Small 9:413

18. Shang L, Nienhaus GU (2012) Gold nanoclusters as novel optical probes for in vitro and in vivo fluorescence imaging. Biophys Rev 4:313

19. Chevrier DM, Chatt A, Zhang PJ (2012) Properties and applications of protein-stabilized fluorescent gold nanoclusters: short review. J Nanophoton 6:064504

20. Tran ML, Zvyagin AV, Plakhotnik T (2006) Synthesis and spectroscopic observation of dendrimer-encapsulated gold nanoclusters. Chem Commun 95:2400

21. Pu KY, Luo Z, Li K, Xie JP, Liu B (2011) Energy transfer between conjugated-oligoelectrolyte-substituted poss and gold nanocluster for multicolor intracellular detection of mercury Ion. J Phys Chem C 115:13069

22. Wu Z, MacDonald MA, Chen J, Zhang P, Jin RC (2011) Kinetic control and thermodynamic selection in the synthesis of atomically precise gold nanoclusters. J Am Chem Soc 133:9670

23. Tang ZH, Ahuja T, Wang SM, Wang GL (2012) Near infrared luminescence of gold nanoclusters affected by the bonding of 1,4-dithiolate durene and monothiolate phenylethanethiolate. Nanoscale 4:4119

24. Kennedy TAC, MacLean JL, Liu JW (2012) Blue emitting gold nanoclusters templated by poly-cytosine DNA at low pH and poly-adenine DNA at neutral pH. Chem Commun 48:6845

25. Fabris L, Antonello S, Armelao L, Donkers RL, Polo F, Toniolo C, Maran F (2006) Gold nanoclusters protected by conformationally constrained peptides. J Am Chem Soc 128:326

26. Lin YH, Tseng WL (2010) Ultrasensitive sensing of Hg^{2+} and CH$_3$Hg$^+$ based on the fluorescence quenching of lysozyme type VI-stabilized gold nanoclusters. Anal Chem 82:9194

27. Wen F, Dong YH, Feng L, Wang S, Zhang SC, Zhang XR (2011) Horseradish peroxidase functionalized fluorescent gold nanoclusters for hydrogen peroxide sensing. Anal Chem 83:1193

28. Liu CL, Wu HT, Hsiao YH, Lai CW, Shih CW, Peng YK, Tang KC, Chang HW, Chien YC, Hsia JK, Cheng JT, Chou PT (2011) Insulin-directed synthesis of fluorescent gold nanoclusters: preservation of insulin bioactivity and versatility in cell imaging. Angew Chem Int Edt 50:7056

29. Guevel XL, Hotzer B, Jung G, Hollemeyer K, Trouillet V, Schneider M (2011) Formation of fluorescent metal (Au, Ag) nanoclusters capped in bovine serum albumin followed by fluorescence and spectroscopy. J Phys Chem C 115:10955

30. Yue Y, Liu TY, Li HW, Liu ZY, Wu YQ (2012) Microwave-assisted synthesis of BSA-protected small gold nanoclusters and their fluorescence-enhanced sensing of silver(I) ions. Nanoscale 4:2251

31. Guevel XL, Daum N, Schneider M (2011) Synthesis and characterization of human transferrin-stabilized gold nanoclusters. Nanotechnology 22:275103

32. Xavier PL, Chaudhari KP, Verma K, Pal SK, Pradeep T (2010) Luminescent quantum clusters of gold in transferrin family protein, lactoferrin exhibiting FRET. Nanoscale 12:2769

33. Kawasaki H, Yoshimura K, Hamaguchi K, Arakawa R (2011) Trypsin-stabilized fluorescent gold nanocluster for sensitive and selective Hg^{2+} detection. Anal Sci 27:591

34. Kawasaki H, Hamaguchi K, Osaka I, Arakawa R (2011) ph-dependent synthesis of pepsin-mediated gold nanoclusters with blue green and red fluorescent emission. Adv Funct Mater 21:3508

35. Chen Y, Wang Y, Wang CX, Li WY, Zhou HP, Jiao HP, Lin Q, Yu C (2013) Papain-directed synthesis of luminescent gold nanoclusters and the sensitive detection of Cu^{2+}. J Colloid Interf Sci 396:63

36. Shamsipur M, Molaabasi F, Shanehsaz M, Moosavi-Movahedi AA (2015) Novel blue-emitting gold nanoclusters confined in human hemoglobin, and their use as fluorescent probes for copper(II) and histidine. Microchim Acta 182:1131

37. Mu XY, Qi L, Dong P, Qiao J, Hou J, Nie ZX, Ma HM (2013) Facile one-pot synthesis of L-proline-stabilized fluorescent gold nanoclusters and its application as sensing probes for serum iron. Biosens Bioelectron 49:249

38. Baughman TA (2006) Elemental mercury spills. Environ Health Perspect 114:147

39. Wang ZD, Lee JH, Lu Y (2008) Highly sensitive "turn-on" fluorescent sensor for Hg^{2+} in aqueous solution based on structure-switching DNA. Chem Commun 45:6005

40. Wu GW, He SB, Peng HP, Deng HH, Liu AL, Lin XH, Xia XH, Chen W (2014) Citrate-capped platinum nanoparticle as a smart probe for ultrasensitive mercury sensing. Anal Chem 86:10955

41. Yuan X, Yeow TJ, Zhang QB, Lee JY, Xie JP (2012) Highly luminescent Ag$^+$ nanoclusters for Hg^{2+} ion detection. Nanoscale 4:1968

42. Lu DT, Zhang CH, Fan L, Wu HJ, Shuang SM, Dong C (2013) A novel ratiometric fluorescence probe based on BSA assembled silver nanoclusters for mercuric ion selective sensing. Anal Methods 5:5522

43. Ding H, Li HW, Liu PC, Hiltunen KJ, Wu YQ, Chen ZJ, Shen JC (2014) Templated in-situ synthesis of gold nanoclusters conjugated to drug target bacterial enoyl-ACP reductase, and their application to the detection of mercury ions using a test stripe. Microchim Acta 181:1029

44. Oskoei YM, Bagheri N, Hassanzadeh J (2015) Ultrasensitive determination of mercury(II) using a chemiluminescence system composed of permanganate, rhodamine B and gold nanoprisms. Microchim Acta 182:1635

45. Abdelhamid HN, Wu HF (2015) Reduced graphene oxide conjugate thymine as a new probe for ultrasensitive and selective fluorometric determination of mercury(II) ions. Microchim Acta 182: 1609

46. Huang CC, Yang Z, Lee KH, Chang HT (2007) Synthesis of highly fluorescent gold nanoparticles for sensing mercury(II). Angew Chem Int Edt 46:6824

47. Xie JP, Zheng YG, Ying JY (2010) Highly selective and ultrasensitive detection of Hg^{2+} based on fluorescence quenching of Au nanoclusters by Hg^{2+}–Au^+ interactions. Chem Commun 46:961

48. Paramanik B, Bhattacharyya S, Patra A (2013) Detection of Hg^{2+} and F^- ions by using fluorescence switching of quantum dots in an Au-Cluster–CdTe QD nanocomposite. Chem Eur J 19:5980

49. Hu DH, Sheng ZH, Gong P, Zhang PF, Cai LT (2010) Highly selective fluorescent sensors for Hg^{2+} based on bovine serum albumin-capped gold nanoclusters. Analyst 135:1411

50. Zhou RJ, Shi MM, Chen XQ, Wang M, Chen HZ (2009) Atomically monodispersed and fluorescent sub-nanometer gold clusters created by biomolecule-assisted etching of nanometer-sized gold particles and rods. Chem Eur J 15:4944

51. Zhao F, Zhao Y, Liu Y, Chang X, Chen C, Zhao Y (2011) Cellular uptake, intracellular trafficking, and cytotoxicity of nanomaterials. Small 7:1322